

# Performance based design of 300 meter high building

**Kiyoaki Hirakawa, Toshimoto Maeno & Kazuhiro Saburi**  
*Takenaka Corporation*



## SUMMARY

This report introduces a case of full-scale performance based design on which we launched to ensure redundancy and establish new specifications, in designing a 300 meter high skyscraper expected to be the tallest building in Japan, an earthquake-ridden country. The article deals with the backgrounds of the performance based design: the necessity of diverse seismic and the application of new techniques to realize this building.

## Keywords

*performance based design, input earthquake motions, seismic design criteria, redundancy.*

## 1. OUTLINE OF BUILDING AND STRUCTURE

The project discussed in this report is reconstruction of Kintetsu Department Store situated in Osaka City. Figure 1.1 shows the northwest view rendering, and Figure 1.2 shows the east-west sectional view. The Tower will rise 60 stories above the ground and 5 underground stories with a one story penthouse, and house an M&E machine room, a connection to the railway and a parking space on the basement floors, the department store on the lower floors, an art museum, lobbies and offices on the medium level floors, and a hotel and an observatory on the upper floors. Furthermore, the Tower has truss floors between the low-rise and medium-rise structures and medium-rise and high-rise structures and immediately above the high-rise component of the building. Various seismic members and damping members are located at the key points throughout the building.

This building will rise 300 meters and will be the highest building in Japan, while there are many taller buildings all over the world. But because Japan is an earthquake and typhoon-ridden country, the heaviest lateral forces in the world are applied to the design for building in Japan. At the same time, the seismic and wind resistant design criteria of this building is set up higher than usual high-rise buildings .



**Figure 1.1.** Northwest view rendering

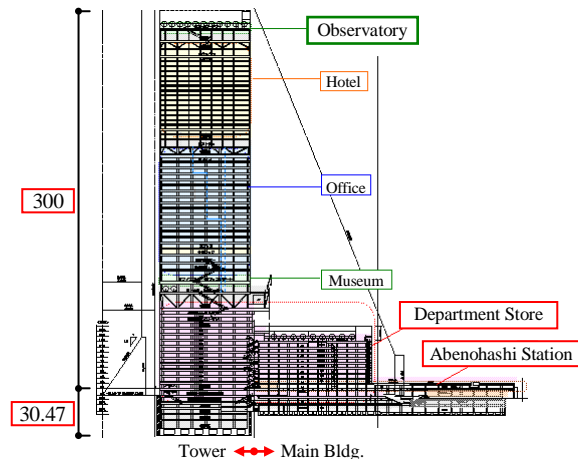


**Figure 1.2.** East-west sectional view

## 2. IMPLEMENTATION OF DIVERSE SEISMIC DESIGNS

### 2.1. Target seismic performance

#### 2.1.1. Design criteria for seismic response analysis (Table 2.1 Design Criteria)

The design of this building is based on the design policy that the design criteria for member conditions established for normal high-rise buildings shall be upgraded by one grade for this building.

**Table 2.1,** Design criteria

Outline of earthquake motions		Level 1	Level 2	Seismic Safety Margin Analysis Level
		- Rare. - Recurrence interval: Approx. 50 years	- Very rare. - Recurrence interval: Approx. 500 years	- 1.5 times stronger than the Notification Level-2.
Target building performance		Continuously usable	Repairable	Repairable (Reinforceable)
Super-structure	Story drift angle	$5.00 \times 10^{-3}$ rad.	$10.00 \times 10^{-3}$ rad.	$13.50 \times 10^{-3}$ rad.
	Ductility factor of story	Allowable stress for short-term loading, or less	1.0 or less	2.0 or less
Substructure	Underground frame / foundation	Allowable stress for short-term loading, or less	Less than ultimate strength	Underground frame: Ductility factor of members < 4.0 Foundation/piles: Ultimate strength or less
	Pile bearing capacity	Allowable bearing capacity for short-term loading, or less	Allowable bearing capacity for short-term loading, or less	Ultimate bearing capacity, or less

#### 2.1.2. Design criteria for members

The design criteria for members are shown below in Table 2.2. Columns and trusses are not allowed to be plastically deformed under the earthquake motions even at the Seismic Safety Margin Analysis Level. Girders and braces are not allowed to be plastically deformed under the earthquake motions up to the Level 2 but allowed at the Seismic Safety Margin Analysis Level.

**Table 2.2,** Potential loads and safety decision criteria in designing superstructure members

Area	Level 1	Level 2	Seismic Safety Margin Analysis Level
	Functions maintained. Hardly damaged. Repair hardly required.	Major functions secured. Minor damaged. Minor repair required.	Specified functions secured. Moderately damaged. Limit of repair.
	Allowable stress for short-term loading, or less	Less than elastic limit strength or ultimate strength	Less than ultimate strength, or partially plastically deformed.
Column	Allowable stress for short-term loading, or less	Less than ultimate strength	Less than ultimate strength
Girder	Allowable stress for short-term loading, or less	Less than ultimate strength	Plastic hinges allowed.
Brace	Allowable stress for short-term loading, or less	Less than ultimate strength	Plastic hinges allowed.
Truss	Allowable stress for short-term loading, or less	Less than elastic limit strength	Less than ultimate strength
Steel plate wall	Not shear yielded.	Allowed to be shear yielded.	Allowed to be shear yielded.
Friction damper	Allowed to be slide rotated.	Allowed to be slide rotated.	Allowed to be slide rotated.
Earthquake-resisting wall	Allowable stress for short-term loading, or less	Less than ultimate strength	Less than ultimate strength

## 2.2. Study of seismic response analysis results

### 2.2.1. Seismic response analysis model and eigenvalue analysis

The basic principles of the seismic response analysis against horizontal motions are as follows. The analysis model is illustrated in Figure 2.1.

- 1) The earthquake motions shall be input at the 5th basement level foundation bed.
- 2) The bending stiffness component is elastic, and the shear stiffness component is elasto-plastic.
- 3) The internal viscous damping of the structure shall be considered as the Rayleigh's damping in which the damping ratio for the primary and secondary modes is set to 2%. The damping of the ground shall be considered only in the rocking vibration, not in the swaying vibration.

Table 2.3 shows the natural periods in the eigenvalue analysis.

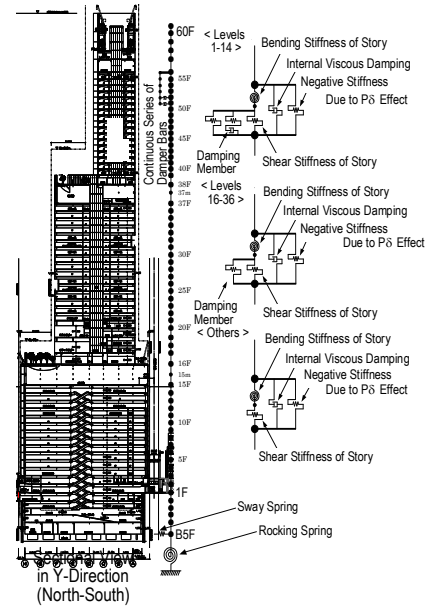


Figure 2.1 View of analysis model

Table 2.3. Natural periods (in seconds)

Direction	First	2nd	3rd	4th	5th	Direction	First	2nd	3rd	4th	5th
X	5.64	2.31	1.38	0.92	0.76	Y	5.77	2.39	1.31	0.85	0.69

### 2.2.2. Input earthquake motions

The input earthquake motions in the response analysis are categorized into three types as shown below in Table 2.4: (1) the Notification Waves and Standard Waves for legally-required design purpose; (2) the Notification Waves created for the seismic safety margin analysis level of maximum class earthquake motions by increasing by half the bedrock waves for the Level-2 Notification Waves; and (3) the earthquake motions intended for study in consideration of regionality. Figures-2.2 and -2.3 show the velocity response spectra against the input earthquake motions (References: [Inkura, 1986; Prefecture of Osaka, 2007; City of Osaka, 1997]).

Table 2.4. Input earthquake motions for design purpose and seismic safety margin analysis

		Level 1		Level 2		Seismic Safety Margin Analysis Level	
		Vmax (mm/s)	Amax (mm/s <sup>2</sup> )	Vmax (mm/s)	Amax (mm/s <sup>2</sup> )	Vmax (mm/s)	Amax (mm/s <sup>2</sup> )
Standard Waves	Elcentro 1940 NS	(1) 250	2,555	500	5,110	—	—
	TAFT 1952 EW	250	2,485	500	4,970	—	—
	Hachinohe 1968 NS	250	1,669	500	3,338	—	—
Notification Waves	Notification Wave A	76	552	379	2,517	(2) 528	3,244
	Notification Wave B	109	471	613	1,929	817	2,919
	Notification Wave C	83	497	383	2,098	560	2,604
Regional Waves	Nankai earthquake NS	(3) —	—	210	863	—	—
	Nankai earthquake EW	—	—	275	987	—	—
	Tonankai/Nankai earthquake NS	—	—	—	—	268	1,213
	Tonankai/Nankai earthquake EW	—	—	—	—	419	1,067
	Uemachi fault zone (UFZ) Case 1 NS	—	—	—	—	329	3,485
	UFZ Case 1 EW	—	—	—	—	813	4,107
	UFZ Case 2 NS	—	—	—	—	291	2,317
UFZ Case 2 EW	—	—	—	—	456	3,269	

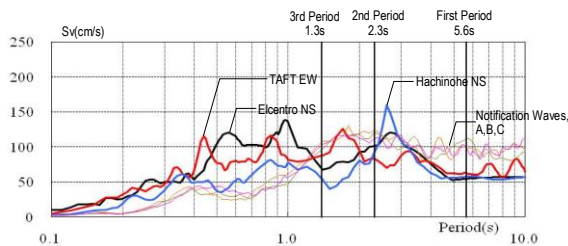


Figure 2.2. Velocity response spectra (level 2, h=0.05)

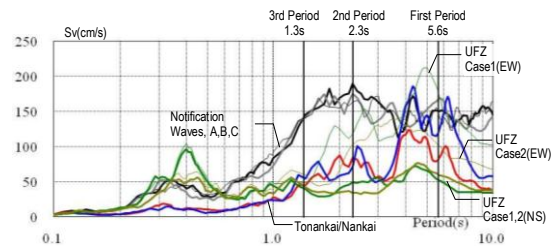


Figure 2.3. Velocity response spectra (regional waves, h=0.05)

### 2.2.3. Results of seismic response analysis

The results of the response analyses against the earthquake motions at the Level 2 and Seismic Safety Margin Analysis Level meet the design criteria. The results of the response analysis against the regional earthquake motions are shown in Figures 2.4 and 2.5.

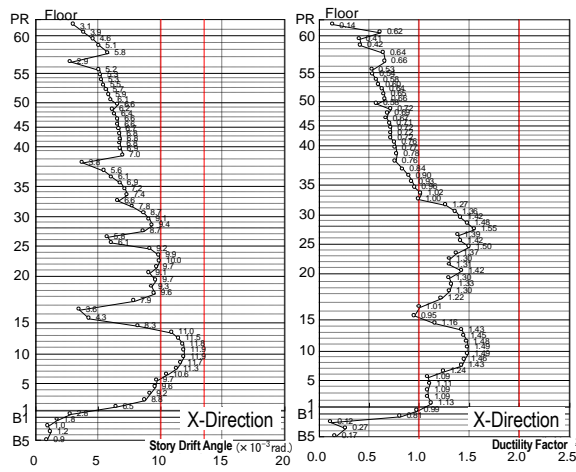


Figure 2.4. Results of response analysis, Tonankai/Nankai Earthquake (max. story drift angles, max. ductility)

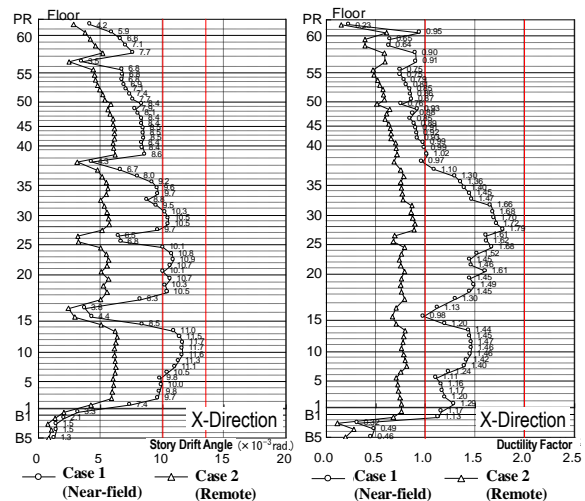


Figure 2.5. Results of response analysis, UFZ Earthquake (max. story drift angles, max. ductility factors)

## 2.3. Study in consideration of variation in input earthquake motions

### 2.3.1. Study on variation in UFZ waves

#### 2.3.1.1. Study in consideration of effects of calculation points

For the input earthquake motions of the UFZ (Uemachi fault zone) in this design, the surface wave at the calculation point near the construction site is used for the response analysis, out of many calculation points (output points) on the fault line shown in Figure 2.6. The effects of the input earthquake motions calculated at the other calculation points are studied here as the means of obtaining redundancy of the seismic performance. Figure 2.7 shows the velocity response spectra (h=5%) on the free engineering bedrock at all the calculation points. Figure 2.8 shows the results of the seismic response analysis: The magnitude and period characteristics of earthquake motions vary according to the calculation points, which causes the responses to be changed, but their values are nearly equal to the criteria at the Seismic Safety Margin Analysis Level.

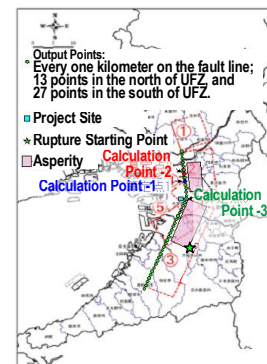


Figure 2.6. Locations of calculation points

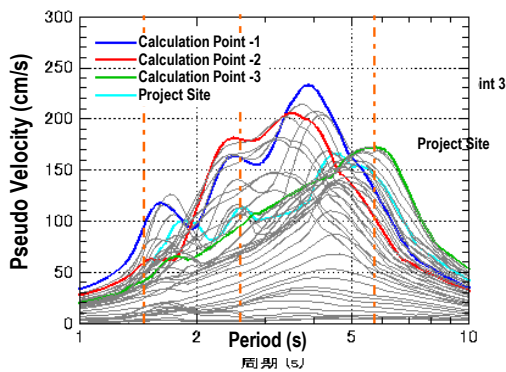


Figure 2.7. Velocity response spectra

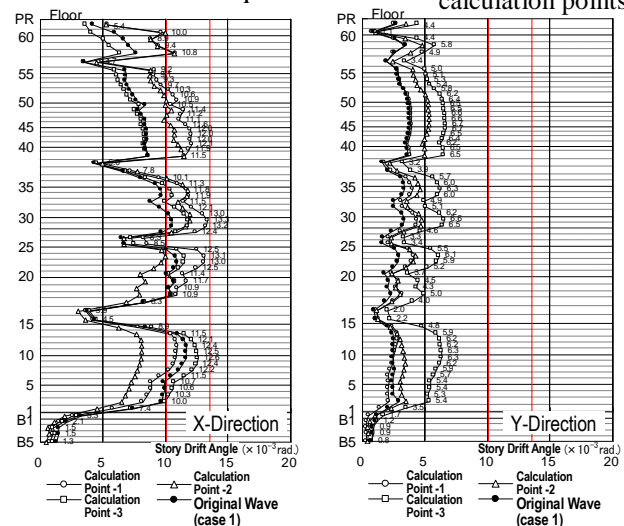


Figure 2.8. Study on variation in UFZ (1) (max. story drift angles)

2.3.1.2. Study on effects of higher-order modes (second/third order modes)

The predominant period of the UFZ earthquake motions created as the regional waves was found to be the value close to the first natural period of the projected building. Additionally, the response analysis was conducted under the Uemachi earthquake waves that have the predominant period almost equal to the second or third natural period of the building, and their effects were reviewed. Since the earthquake motions of the waves for the second and third mode analyses were large, the maximum value of story drift angle response was found to be 1/52, which does not meet the requirement at the Seismic Safety Margin Analysis Level (1/75) but is acceptable in this study on variation.

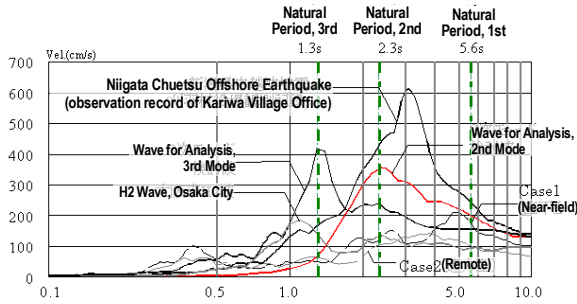


Figure 2.9. Velocity response spectra

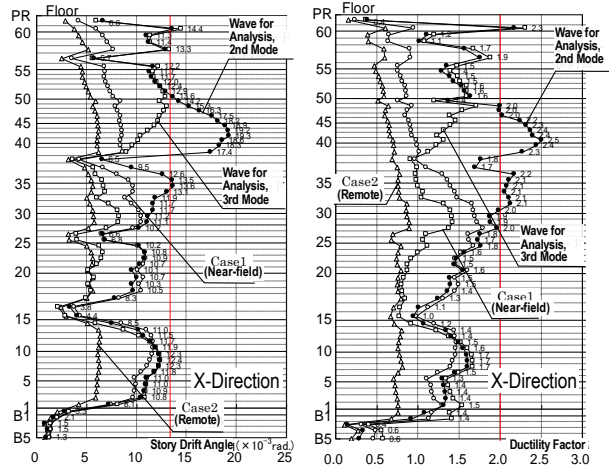


Figure 2.10. Study on variation in UFZ (2) (story drift angles and ductility factors)

2.3.2. Study on variation in Tonankai/Nankai earthquake waves

In order to study the effects of the variation in the ocean earthquake motions, the time interval of the applied earthquake motion waveform data was adjusted, and the predominant period of the earthquake motions was caused to agree with the first natural period of the building, the effects of which were studied. According to the following figures, the maximum response values are increased by approx.20-30% when the predominant period is in agreement with the first period.

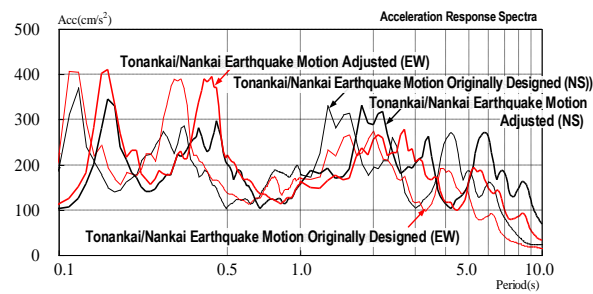


Figure 2.11. Acceleration response spectra

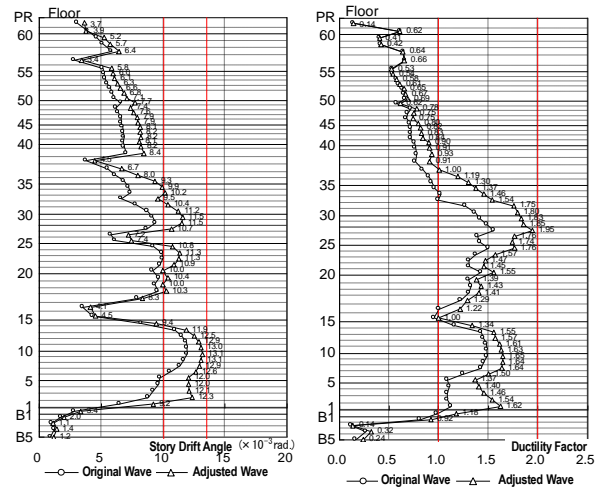


Figure 2.12. Study on variation in Tonankai/Nankai Earthquake motions (story drift angles & ductility factors)

2.4. Conclusion on seismic design

In designing a 300-meter high tower building, we conducted the following various studies to ensure sufficient safety and redundancy (1) establishing the seismic design criteria upgraded by one grade than usual; (2) reviewing the mechanism in static analysis; (3) study on the earthquakes at Seismic Safety Margin Analysis Level; (4) response analysis against regional earthquake waves; (5) study on variation in regional seismic waves; and (6) study in consideration of variation in analysis conditions.

### 3. APPLICATION OF NEW TECHNIQUES

#### 3.1. CFT columns using high-strength materials

##### 3.1.1. Introduction

Concrete filled steel tube (“CFT”) columns made of high-strength concrete  $F_c150$  and high-strength steels equivalent to the yield strength  $440 \text{ N/mm}^2$  and tensile strength  $590 \text{ N/mm}^2$  are used in this building in order to ensure the safety of the columns that bear high axial forces. They are out of the applicable scope of the Japanese guideline as shown in Figure 3.1.

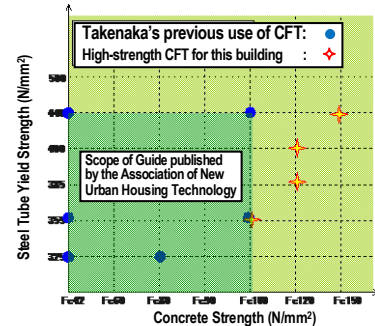


Figure 3.1 Scope of Guide

##### 3.1.2. Verification of deformation capacity

In the loading test (Figure 3.2) performed prior to the design, we increased the axial force from  $0.70 cNu$  ( $cNu$ : compressive axial load capacity) to  $0.5 Nt$  ( $Nt$ : tensile axial load capacity) in proportion to shearing forces. Consequently, the deformation capacity equivalent to the value at the member's angle around  $10/1000 \text{ rad.}$  was identified as shown in Figure 3.3.

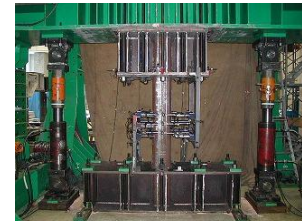


Figure 3.2. View of test

##### 3.1.3. Analysis of bending ultimate strength

The experimental value can be evaluated if the concrete strength is multiplied by the strength reduction factor ( $cru=0.70$ ) as shown in Figure 3.4 because the shape of the concrete stress block assumed in the accumulative strength equation with fully-plastic moment is not square as shown in Figure 3.5.

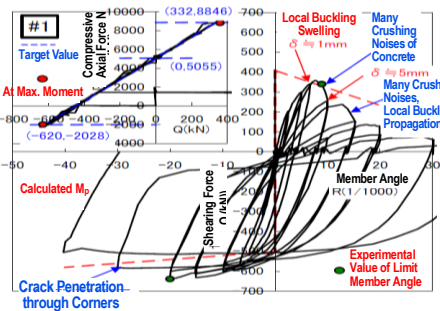


Figure 3.3. Load-deformation relations

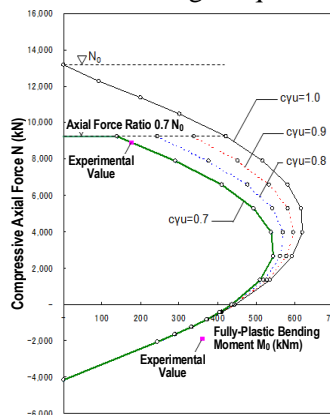


Figure 3.4. M-N correlations

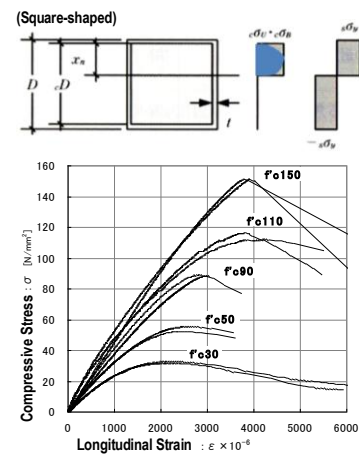


Figure 3.5. Load-strain relations of concrete

##### 3.1.4. Design conditions for CFT columns

The sectional design conditions for CFT columns are shown below in Table 3.1.

Table 3.1. Design conditions

	Against story shear force for design	Against Level 2 earthquake
Transfer of axial forces	To be designed with the bearing forces of <b>horizontal plates.</b>	To be designed with the bearing forces of <b>horizontal plates.</b>
Designing of bending and axial forces	No more than the allowable stress for short-term loading by adding concrete and steel tube strengths (the allowable stress calculated by using the yield strain of the steel tube or concrete, whichever is smaller).	Under the ultimate strength only by adding concrete and steel tube strengths. <b>Apply the compressive concrete strength reduction factor</b> to concrete of $F_c 100 \text{ (N/mm}^2\text{)}$ or more.
Axial force ratio	$N \leq \frac{1}{3} cA \cdot F_c + \frac{2}{3} sA \cdot s_f c$	$\frac{N}{N_0} \leq 0.7$

### 3.2. New joint system

#### 3.2.1. Introduction

This building uses a new joint system consisted of outer diaphragm and aluminum spray jointing.

#### 3.2.2. Outer diaphragm

The outer diaphragm employed in this building is a split type as shown in Figure 3.6 and oblique-fillet welded with a column. A horizontal force application test was performed on a partial frame jointed with a beam by aluminum spray jointing, and as the result, it yielded at the bolts, by which it was verified that it has a sufficient deformation capacity equivalent to about  $40p$  (Fig 3.7, 3.8 [Matsuo et al., 2010]).

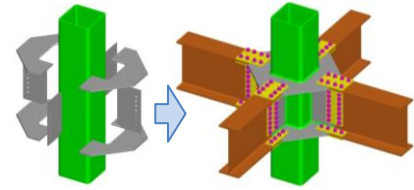


Figure 3.6. Split outer diaphragm

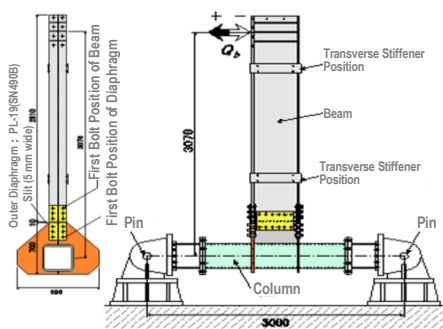


Figure 3.7. Test article - outer diaphragm

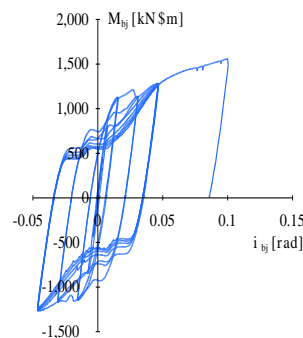


Figure 3.8. Load-deformation relations

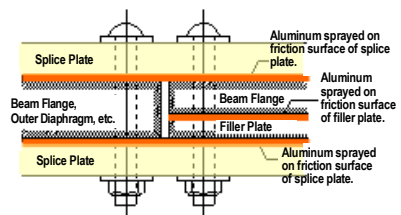


Figure 3.9. Aluminum spray jointing

#### 3.2.3. Aluminum spray jointing

Aluminum was sprayed on the surface of the splice plate at each beam flange bolt joint that is in contact with the base material as shown in Figure 3.8. The jointing method with the slip factor improved to 0.70 is used to reduce the quantity of bolts and the size of splice plates. The following conditions were established to keep the slip factor 0.70.

- (1) Spraying method: arc
- (2) Sprayed coating thickness: 300  $\mu\text{m}$  or more
- (3) Splice plate thickness: 12mm or more
- (4) Friction treatment surface: blasting
- (5) Splice plate base treatment: blasting to remove black scale
- (6) Allowable lap gaps: 1.0 mm or less

We also provided construction troubles on purpose and grasped their effects on the slip factors (Figure 3.10 and Figures 3.11 to 3.13) (Architectural Institute of Japan, 2009).

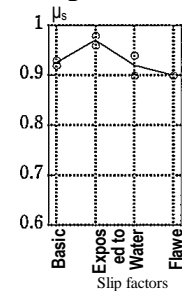


Figure 3.10 Relations between construction troubles and slip factors



Figure 3.11. Base material soaked in water



Figure 3.12. Flawed test articles: Direction orthogonal to force application

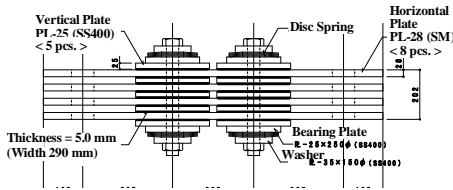


Figure 3.13. Oil-stained leather glove test: Oil-stained leather glove

### 3.3. Dampers

#### 3.3.1. Rotational friction dampers

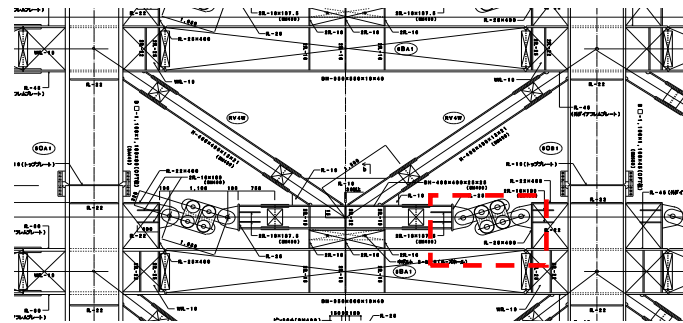
A rotational friction damper generates a given frictional force via the friction pads each sandwiched between horizontal and vertical steel plates, which are bolted together, as shown in Figure 3.14.



**Figure 3.14.** Upper profile of rotational friction damper



**Figure 3.15.** Front elevation of rotational friction damper



The result of the full-scale test has verified that the deformation performance was very stable as shown in Figure 3.16. In this building, three types of rotational friction dampers, 1500KN, 2000KN and 2250KN, that number 108 dampers in total are installed around the department store's core of the low-rise component. Their friction forces are not more than the static friction force in strong winds (Level 1), but they started allowing for sliding and producing a vibration suppression effect in a Level-1 earthquake.

Speed dependency test:  $\pm 40$  mm, 0.3 Hz, 75.4 mm/sec., vibration 4 cycles  
Horizontal displacement between clevises (LKG-500) - horizontal loads

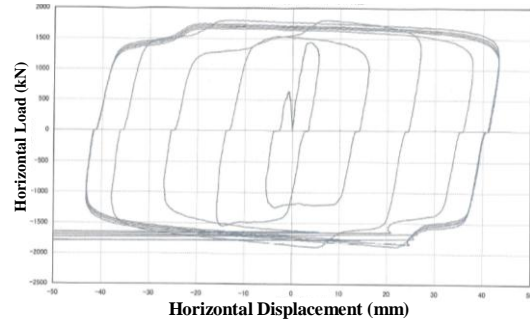


**Figure 3.16.** Load-deformation relations

#### 3.3.2. Corrugated steel plate walls

A corrugated steel plate wall is an earthquake-resisting member consisting of a steel plate corrugated in the direction of the height and the surrounding flanged steel plates that are integrated with their frame (Figure 3.17). The angles arranged with a given spacing restrain buckling as stiffened ribbed plates and reach shear yield at  $R=3/1000$  rad. as shown in Figure 3.18. They display high plastic deformation performance until they are buckled at  $R=30/1000$  rad., and absorb seismic energy. We also calculated the marginal scale factor of cumulative plastic deformation from the fragility curves shown in Figure 3.19 that were based on the fatigue test results. Then it was confirmed that it exceeded the scale factors of cumulative plastic deformation of the walls that we calculated from the earthquakes experienced during the in-service period of this building.

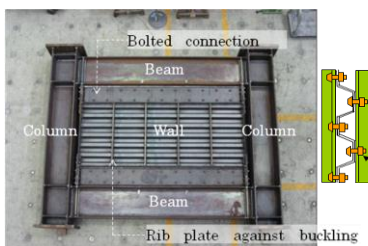


**Figure 3.17.** Corrugated steel

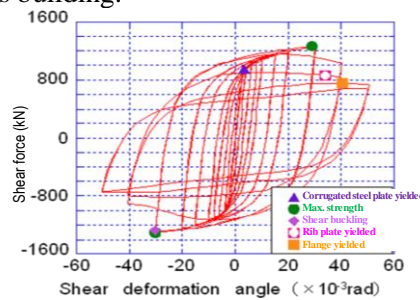


**Figure 3.18.** Load-deformation relations of corrugated steel plate

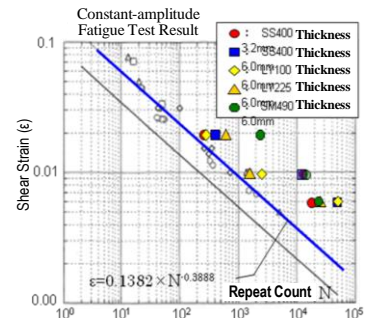


**Figure 3.19** Fatigue test results

### 3.3.3. Inverted-pendulum ATMD

The hat truss floor is equipped with mass dampers that operates only in the north-south (narrow side) direction, one each at the west and east ends of the building as shown in Figure 3.21 for the purpose of improving the habitability of the hotel in strong winds. Dampers work only when their period is synchronized with the natural period of the building which is as long as about 6 seconds. The length of the conventional suspended pendulum has to be extremely long for that purpose but can be minimized by combining it with an inverted pendulum (Figure 3.20).



Figure 3.20.

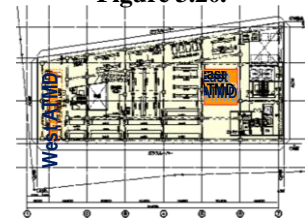


Figure 3.21. ATMD layout

### 3.4. Foundation structure system

A piled raft foundation consisting of piles and bottom plate both of which bear the building load is used for this building, where an inverted placing method is applied, using basement columns. Therefore, the superstructure is constructed up to about the 50th floor level prior to the bottom plate installation. Accordingly, the piles bear as much as about 90% of the column axial forces, and the bottom plate bears the remaining forces (only about 10%). One pile is located per column as shown by the pile plan in Figure 3.22, but the existing building frame is buried in the circumference, which makes it difficult to drive piles. Consequently, the SMW (soil mixing wall) construction method is used. As shown in Figure 3.23, the column axial forces are transferred to the core steel of the soil cement retaining walls through the headed studs from the exterior wall of the basement, and finally transferred to the ground. The SMW method is environmentally friendly because about 50% of the soil can be reused.

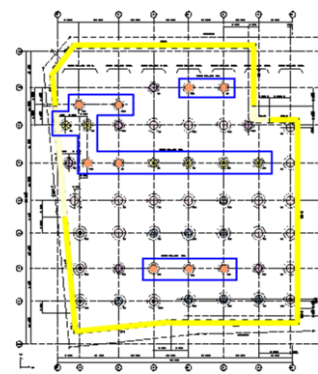


Figure 3.22. Pile plan

## 4. CONCLUSION

In conducting the performance based design of this building, we established new design criteria for the seismic design that ensures redundancy and also performed redundancy-conscious tests to establish the specifications of various new techniques. Thus we were able to realize the performance based design of Japan's tallest building by taking not single but multidimensional approaches to unknown matters.

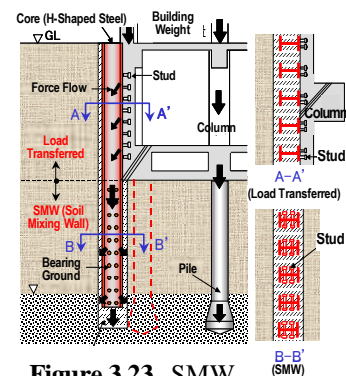


Figure 3.23 . SMW

## REFERENCES

- Architectural Institute of Japan, Sliding factor and relaxation characteristics of friction joints of aluminum sprayed splice plates with high-tension bolts, Summaries of technical papers of Annual Meeting Architectural Institute of Japan, August 2009.
- City of Osaka, Report of Investigation meeting on earthquake measures for Osaka City public works and buildings, March 1997.
- Irikura, K, Prediction of strong acceleration motions using empirical Green's function, Proc. 7th Japan Earthq. Eng. Symp., pp. 151-156, 1986.
- Matsuo, M; Saburi, K; Tanaka, T; and Inoue, I, Partial frame test on beam joining area of H-shaped section of square steel tube column in split-type outer diaphragm system, Structural papers of Architectural Institute of Japan, February 2010.
- Prefecture of Osaka, Report on investigation into comprehensive measures for natural-disaster prevention (earthquake damage estimation), Osaka Prefecture, March 2007.